International Journal of Nanoelectronics and Materials
IJNeaM
ISSN 1985-5761 | E-ISSN 2232-1535

Synthesis of In_2O_3 nanoparticles decorated multi-walled carbon nanotubes by laser ablation in liquid and their characterization

Hawraa M. Abdul-Redaa [a], Khawla S. Khashan [b] *, Aseel A. Hadi [b], and Haleema Sadia [c]

[a]*Department of Laser and Optoelectronics Engineering, University of Technology - Iraq*
[b]*Department of Applied Sciences, University of Technology – Iraq*
[c]*Manchester Institute of Education, University of Manchester, UK*
* *Corresponding author. E-mail: khawla.s.khashan@uotechnology.edu.iq; ORCID: 0000-0001-9028-919*

Received 09 July 2024, Revised 28 October 2024, Accepted 07 November 2024

ABSTRACT

Here, we report the application of the pulsed Nd: YAG-laser ablation technique (PLA) to the decoration of In_2O_3 nanoparticles (NPs) on Multi-Wall Carbon Nanotubes (MWCNTs). Nanocrystalline indium oxide particles were prepared for the first time by direct interaction of indium target with different laser energy for 100 pulses. We could regulate how much the nanoparticles covered the MWCNTs surface by applying the number of laser ablation pulses 50, 75, 100, and 125 at 550 mJ. A Q-switched Nd: YAG laser (1064 nm) with a 9 ns pulse width was used to accomplish the ablation process. The absorption spectra of the pure In_2O_3 NPs and decorated nanotubes showed a prominent peak at about 275 nm and 265 nm, respectively. It is discovered that the band energy of the prepared samples is laser parameters dependent. It was decreased with increasing the laser energy for pure In_2O_3 NPs and decreased with increased laser shots for In_2O_3@MWCNTs nanostructure. X-ray diffraction analysis demonstrated the presence of CNTs and In_2O_3 nanoparticles phases. The Photoluminescence spectra (PL) peak emission of In_2O_3@MWCNTs nanostructure was in the visible region and lower intense than that of In_2O_3 nanoparticles. Energy-dispersive spectra showed the presence of C, O, and indium in the final product. The results showed that adding In_2O_3 NPs to the surface of MWCNTs is a viable way to improve wideband light absorption. This approach also offers more effective charge transfer with the lowest effective recombination rate, which improves photocatalytic performance and may find use in optoelectronic devices.

Keywords: *Indium oxide (In_2O_3), Laser ablation in liquid, In_2O_3@MWCNTs, Heterostructures, MWCNTs*

1. INTRODUCTION

Novel nanostructured materials synthesis has recently attracted great concern because of their rare properties and important potential applications [1]. In recent years, colloidal semiconductor metal nanoparticles (NPs) attracted great interest as candidates for light-emitting diodes and photodetectors. Because of their easy fabrication, quantum confinement effect, large active area, low cost, controllable production, low-temperature solution processing and highly efficient electron transport [2-4]. Zinc oxide (ZnO), nickel oxide (NiO), and titanium dioxide (TiO_2) are metal oxide semiconductor nanomaterials with a broad energy gap that find numerous uses in nonlinear optics and optoelectronics. Out of them, In_2O_3 is considered a wide band gap semiconductor n-type metal oxide (Eg = 3.75eV at room temperature) [5].

Indium oxide (In_2O_3) is one of the significant transparent conducting oxides (TCO). In_2O_3 has exceptional properties such as high transparency (>70%) to visible light, low electrical resistivity ~ 10-10 Ω·m, high surface area, ease of electron transfer, high crystallinity, cubic structure with lattice parameters (a = b = c = 10.18 Å), and it interacts strongly with certain gas molecules [6-8]. In_2O_3 plays a key role in different technological applications. The active layer in short-wavelength optoelectronic devices, gas sensors, photocatalytic conversion, UV-Vis photodetectors, solar cells, flat panel displays, thin film transistors, and biosensors are just a few of the applications in which In_2O_3 is essential. [9-11]. This contradiction is because of the complex electronic band structure of In_2O_3. To develop applications of In_2O_3, researchers produce them in numerous forms such as nanowires, nanobelts, nanotubes, and nanoparticles. The properties of nanomaterials depend on the size and shape which is affected by the synthesis methods [12]. Several physical and chemical techniques have been employed to synthesis Indium oxide nanoparticles including Sono-chemical, sputtering, electrochemical deposition, sol gel, evaporation, atomic layer deposition [13, 14]. Among them, the pulsed laser ablation in liquid method has become popular because of the excellent properties of the produced nanomaterials [15, 16].

PLA is a technique using outstanding laser beam density to produce the cavitation bubble of plasma from the bulk-target surface. To create the required nanomaterials, the liquid can quickly quench and dilute the generated plasma [17]. This technique is only suitable for producing precursor nanoparticles since laser energy, a gradient form, stimulates a wide size distribution during nanoparticle creation [18].

This technique has several advantages include its simplicity, which makes it inexpensive, effective, and free of chemical substances. It also produces free-contamination nanoparticles without causing environmental pollution [18].

Carbon nanotubes (CNTs) have garnered large attention Due to their superior structural, electrical, and mechanical qualities [19]. CNTs molecular weight is hard to define because the chemistry of their surface is complicated, induced by multiple modification processes, and their broad length distribution as well, they desired to disperse in water when being treated as detective molecules [20]. They have a high surface area, low density, mechanical strength, high chemical stability, and high electrical and thermal conductivity [21]. Due to the remarkable photoluminescent properties such as excitation power and the superior light emission stability at temperature, CNTs are the major candidates for excellent characteristics active photonics devices. Optical devices based on them are visible light range waveguides and sensors [22]. Multiwalled carbon nanotubes (MWCNTs) have a large surface area, a unique atomic bonding configuration, and a unique chemical composition due to their external walls and central hollow cores [23].

Combining different materials can generate new materials with novel properties not existing in their counterparts [19]. CNTs decorated with metal oxides are of interest from a technological and fundamental standpoint due to their unique characteristics. This novel material can be used in a wide variety of fields. Since In_2O_3 has a large band gap, it can only absorb and work under UV light; materials based on In_2O_3 require photocatalysis of visible light. It is expected that the combination of In_2O_3 nanoparticles and CNTs will result in a new type of material that can be used as photodetectors in regions with visible radiation.

In the present study, we describe the application of the PLA technique as a simple one-step method to create In_2O_3@MWCNTs nanohybrids by decorating MWCNTs with In_2O_3 NPs. To the best of our knowledge, no research on the PLA-based nano-decoration of MWCNTs with In_2O_3 nanoparticles has been published to date. It is envisaged that these new composite materials will, in various applications, exhibit synergistic physical and chemical properties of the two constituents.

2. EXPERIMENTAL PROCEDURES

2.1. Synthesis of In_2O_3 NPs

Indium metal target in the form of a plate with 99.9% purity and dimensions of (0.5 cm × 0.5 cm) with 1 mm thickness was employed as a target material to produce indium oxide colloid nanoparticles (In_2O_3). The indium plate was put into the bottom of a glass vessel filled with 3 ml of de-ionized water, as seen in Figure 1. A metallic indium target was ablated using a Q-switched pulsed laser beam to create indium oxide nanoparticles. A pulse Q-switched (1064 nm) Nd: YAG laser with a 1 Hz repetition rate, a 9 ns pulse duration, and a 1 mm beam diameter was used to carry out the ablation procedure. The beam of laser was directed onto the in-bulk target surface using a convex lens with a 10 cm focal length to acquire the required energy. Trials at different laser energies about 500-700 mJ were performed with 100 pulses for pure indium oxide nanoparticles and various pulses (50-125) for MWCNTs decorating In_2O_3 nanoparticles.

2.2. Synthesis of In_2O_3@MWCNTs

MWCNTs with a purity of >95%, purchased from PD30L1-5 nano-lab with a diameter of 30±15 nm, and length equal to 1-5 micron. Prior to use, the 1 mg powder of MWCNTs were well dispersed by sonicating them in 3 ml deionized water solution (DDI) for two minutes, producing a suspension with a concentration of 0.3 mg/ml. In_2O_3@MWCNTs was prepared by placing the indium plate in the prepared MWCNTs suspension and then use Nd: YAG pulsed laser with 550 mJ and various numbers of (50, 75, 100, and 125) pulses for the irradiating procedure.

3. CHACTERIZATION OF THE SAMPLES

The spectra of UV-visible absorption for as-prepared In_2O_3 NPs and indium oxide-decorated MWCNTs colloid NPs were recorded in the spectral range of 200-1100 nm and investigated utilizing a dual-beam ultraviolet-visible spectrophotometer (model SP-3000 Plus, OPTIMA). The optical characteristics of the produced In_2O_3 colloidal NPs and In_2O_3-decorated MWCNTs suspension nanostructure were examined via utilizing an optical cuvette cell (quartz) with an optical path of 1 cm. At a diffraction pattern angle of 2θ ranging from 20 to 80 degrees, a Cu-K radiation source (Philips PW) was used to determine the crystal structure of each prepared specimen. X-ray diffraction is a technique used to ascertain the phase of a material. After a solution was dropped onto a glass substrate, the sample for the X-ray assay was ready to be dried in an airtight environment. The Energy Dispersive X-ray (EDX) inspection S50 (FEI company, the Netherlands) was used to determine the chemical composition of the samples that were obtained. The photoluminescence spectra of the In_2O_3 nanoparticles and decorated MWCNTs were evaluated using a

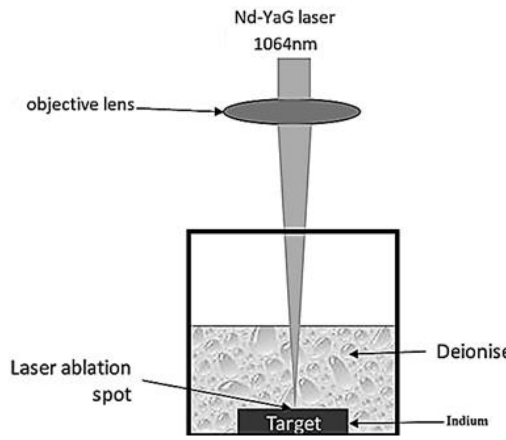

Figure 1. Schematic representation of a laser-ablated indium target in water

fluorescence spectrometer (FLS920) at room temperature, employing an Xe lamp with a wavelength of 320 nm as an excitation source.

4. RESULTS AND DISCUSSION

Figure 2 shows the UV-Vis absorption spectra as a function of the wavelength for In_2O_3 NPs prepared via laser at various laser energies for 100 shots. The spectra demonstrated that the specimens exhibited optical absorption throughout the UV light spectrum. The spectra demonstrated that absorption sharply rises at shorter wavelengths. For wavelengths longer than 275 nm, the absorption line shape does not significantly change as laser energy increases; however, for wavelengths shorter than 300 nm, the intensity of absorption peaks increases with laser energy, with the exception of a higher laser energy of 700 mJ. This is explained as a straightforward rise in the colloid's NP concentration per unit volume, which is consistent with published work [24]. While for higher laser energies, larger particles form and cause a rise in scattering effects. The inter-grain depletion regions caused by the long tail in the absorptance spectra is attributed to Urbach, resulting from inter-grain depletion regions [25].

Figure 3 displays the absorbance spectra of the MWCNTs, both pure and decorated In_2O_3, at different MWCNT decorating concentrations. In_2O_3 NPs have a low visible absorption and a high UV absorption because of their wide band gap [5]. The broad absorbance peak at about 250-265 nm in the optical spectra of the In_2O_3@MWCNTs nanocomposite samples, as shown in Figure 3, is linked to the electronic transitions π-π* of C=C bonds. Furthermore, as the decorating ratio of MWCNTs rises, redshifts to the longer wavelength (red shift) of the nanocomposites' edge are seen in addition to an increase in absorption intensity [1]. This could lead to a deeper comprehension of the basic mechanism through which visible light produces electron/hole pairs [5]. Moreover, In_2O_3@MWCNTs prepared had an absorbance spectrum that was unmistakably higher than In_2O_3 NPs. A high decorating percentage that raises the absorbance peak intensity could be the cause of this. The visible-near infrared regions have also seen a discernible rise in absorption. This implies that the addition of CNTs improves the optical absorption of In_2O_3 NPs.

The energy bandgap (Eg) for the prepared In_2O_3 NPs was estimated using Tauc's relation equation via extrapolating the linear part to the hν-axis of a $(\alpha h\nu)^2$ against photon energy (hν) as illustrated in Figure 4. It is found that Eg depends on laser energy. The band energy decreased with increasing the laser energy, indicates that there were more collisions between the atoms and ions of the vapor, which caused them to congregate inside the ablated plume and ultimately form larger particles. This decrease in Eg agrees with published research [16]. This aligns with the absorbance findings. From the plot of Figure 4, the optical band gap of In_2O_3 NPs was determined to be (3.3, 3.2, 2.9, 2.85, and 2.8 eV) for laser energies of 500, 550, 600, 650, and 700 mJ, respectively.

After decorating with MWCNTs at various laser pulses, it was discovered that the value of the Eg for produced In_2O_3NPs decreases from 3.25 to 2.65 eV, as shown in Figure 5. Increased chemical defects and vacancies in the intergranular regions were brought about by adding MWCNT to the host material. Also, the interaction between In_2O_3 and MWCNTs produced new energy levels to decrease the Eg, are most likely the causes of this decrease in the energy gap created by In_2O_3 NPs addition in In_2O_3 suspension [26]. The decrement in the Eg value proved the bonding formation of In-O-C between In_2O_3 and MWCNTs [27].

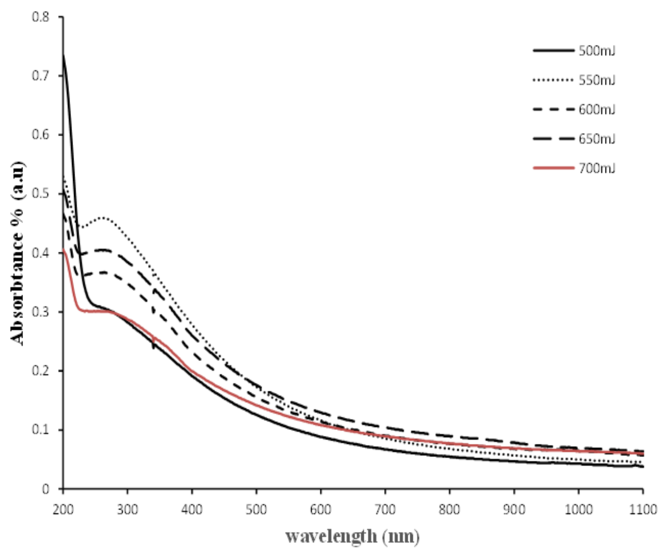

Figure 2. Absorbance spectra of In_2O_3 nanoparticles produced using various laser energies

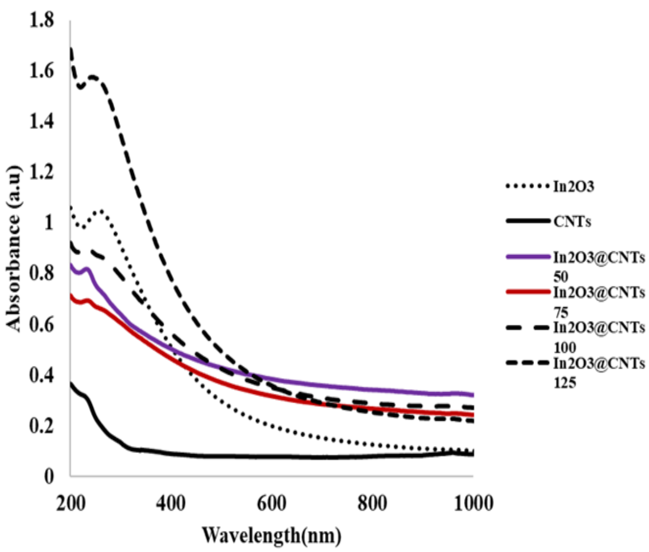

Figure 3. Absorbance spectra of In_2O_3 NPs, MWCNTs, and In_2O_3@MWCNTs nanocomposites

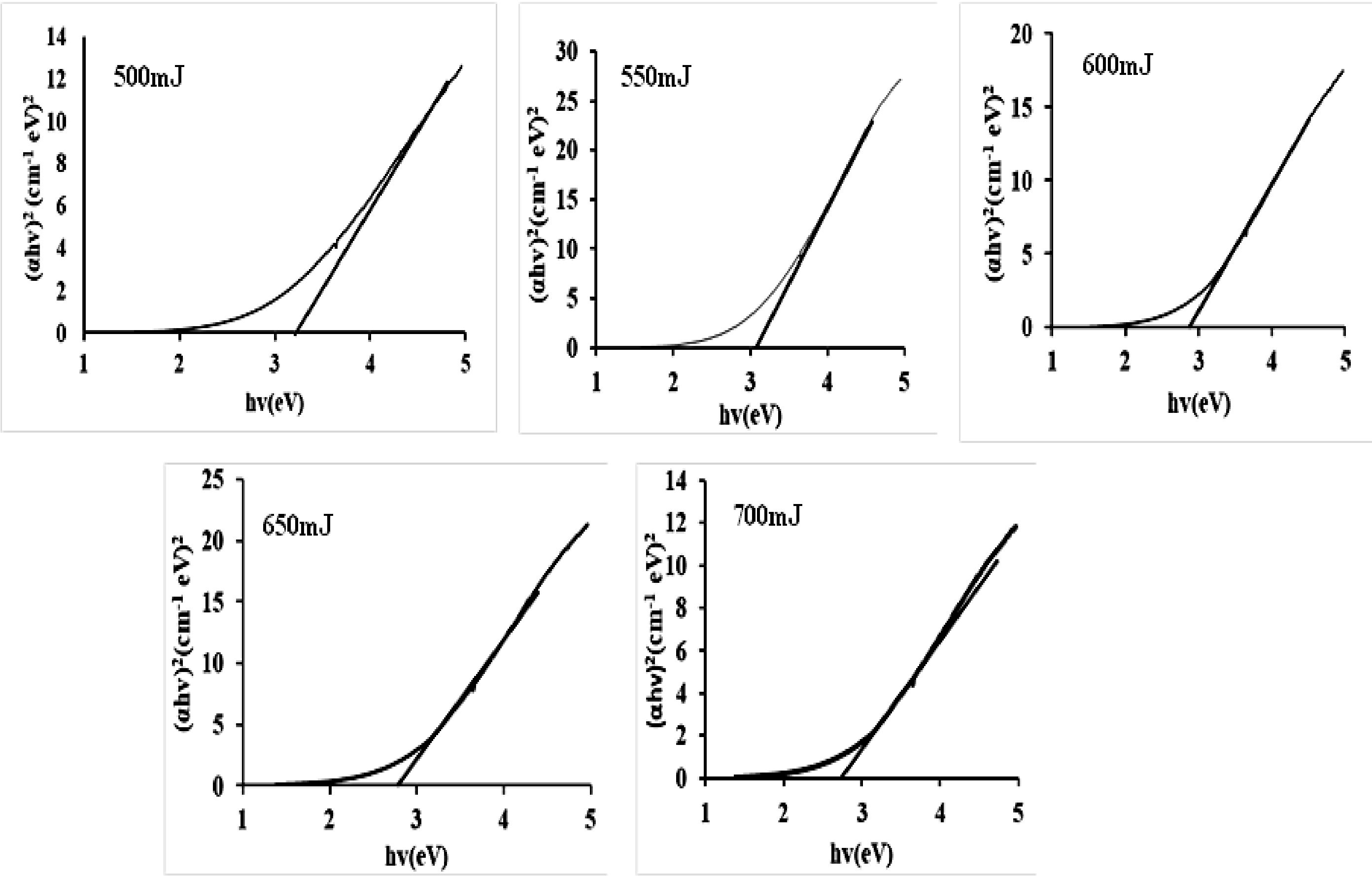

Figure 4. Energy bandgap calculation of In_2O_3 NPs prepared with different laser energies for 100 pulses

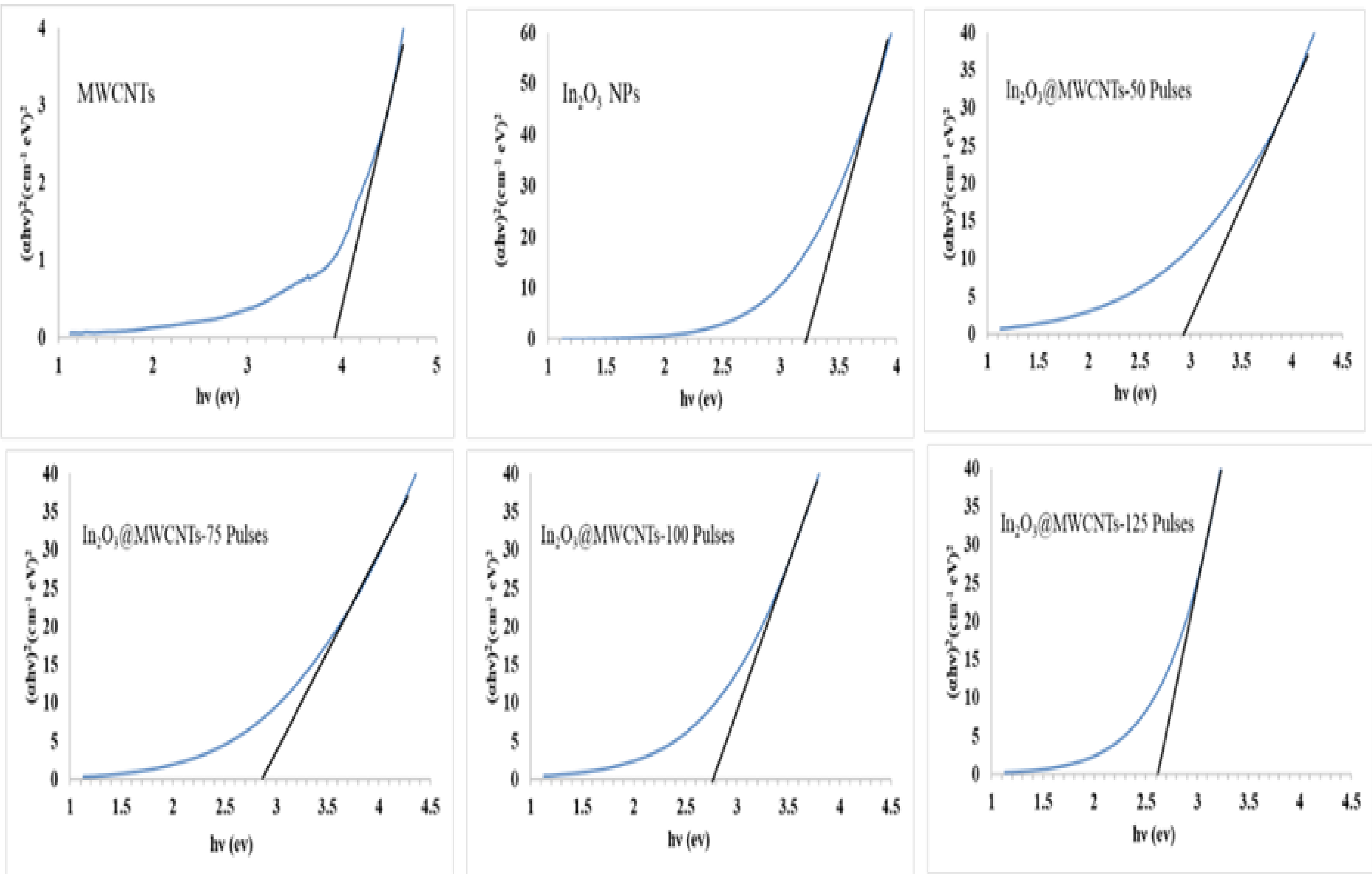

Figure 5. Optical band gap of (a) In_2O_3 NPs, (b) MWCNTs, and (c) In_2O_3 decorated MWCNTs by laser with various laser pulses

Figure 6 shows XRD patterns of In_2O_3 NPs prepared with varying laser energies at 100 pulses. The synthesized nanoparticles are indexed and match the cubic phase of In_2O_3 with a lattice constant of a=10.53 A°, according to the XRD data of In_2O_3 NPs. This is in line with the standard values for bulk cubic-In_2O_3 (JCPDS 6-0416). The In_2O_3 NPs/Glass reveal polycrystalline structures with various orientated crystalline planes such as (222), (321), (400), (420), (511), (521), (600), and (620). The obtained results are consistent with previous studies [28]. The orientation intensity of (In_2O_3/Glass) at 550 and 650 mJ are higher than 500 mJ which may be attributed to good crystallinity. It was revealed that (321) was the preferentially orientated crystal plane. A high degree of crystallization is indicated by the samples' sharp diffraction peaks. Additionally, the pattern showed no additional impurity peaks, indicating the samples' high phase purity.

Figure 7 displays the XRD spectra of pure MWCNTs and In_2O_3/MWCNTs prepared with varying laser pulse counts. It showed low-intensity diffraction peaks at 43.7°, 53°, and 78° and an intense diffraction peak around 2θ = 25.8°. These distinctive peaks show the crystallinity of the MWCNTs and correlate to the carbon of the MWCNTs, which is represented by the (002), (100), (004), and (110) diffraction patterns of typical graphite. This result indicates that MWCNTs have good graphitization. The XRD pattern demonstrated that there were no metal particles or carbonaceous impurities present in the MWCNTs. The XRD patterns of the In_2O_3@MWCNTs samples verified that the peaks were those of In_2O_3 and MWCNT and that the crystallization of the In_2O_3 planes was unaffected by the presence of MWCNTs. The significant peak intensity suggests that the MWCNT surface contains a significant amount of In_2O_3, confirming an appropriate decoration. The carbon peak intensities were very low because of the low concentration of MWCNTs (0.3 mg/ml). The spectrum at orientations (431), (521), and (611) also shows additional peaks that correlate to the In_2O_3 cubic phase. This suggests that crystallinity is enhanced by the addition of CNTs.

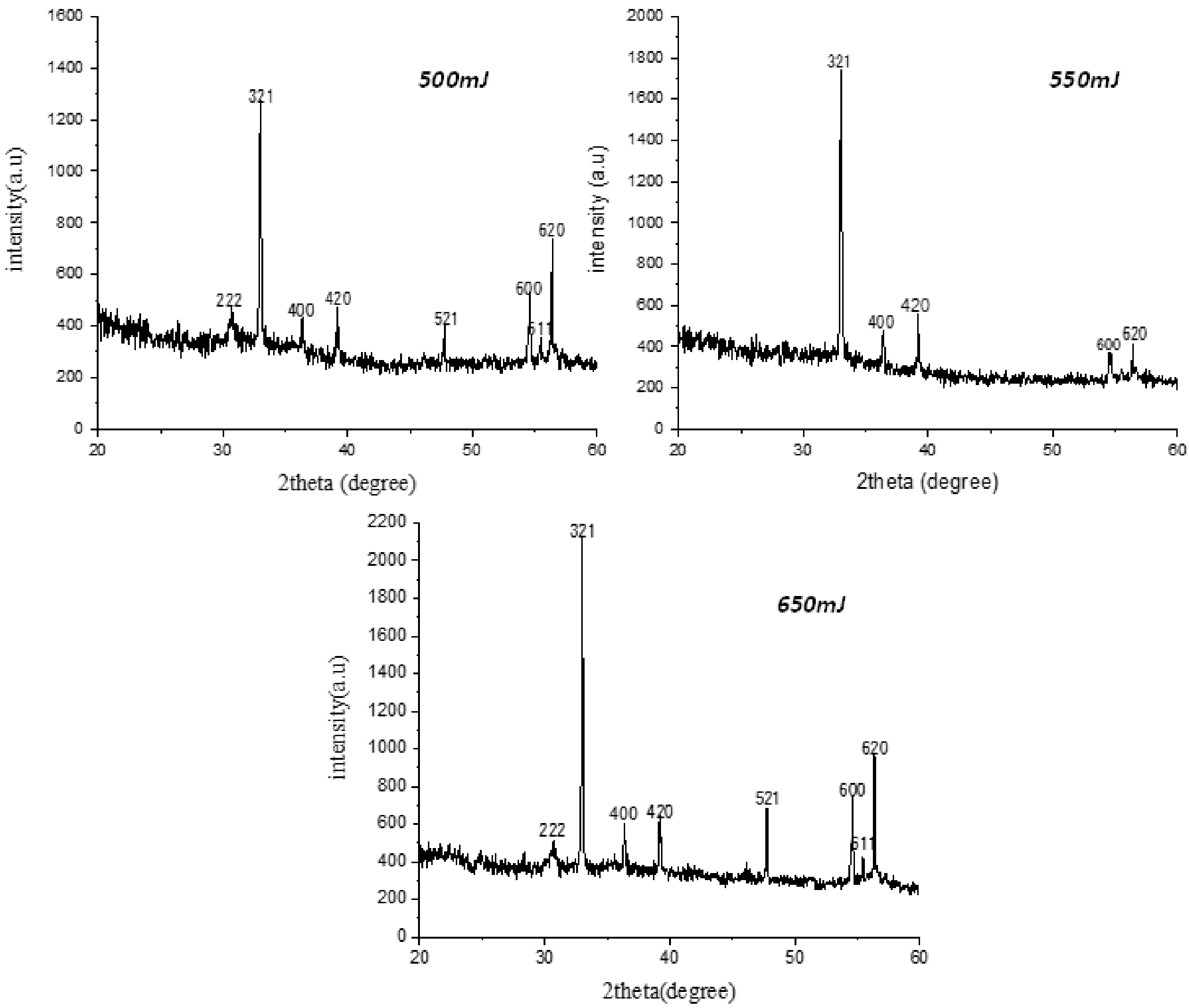

Figure 6. In_2O_3 NPs' XRD patterns after 100 pulses of varying laser energies

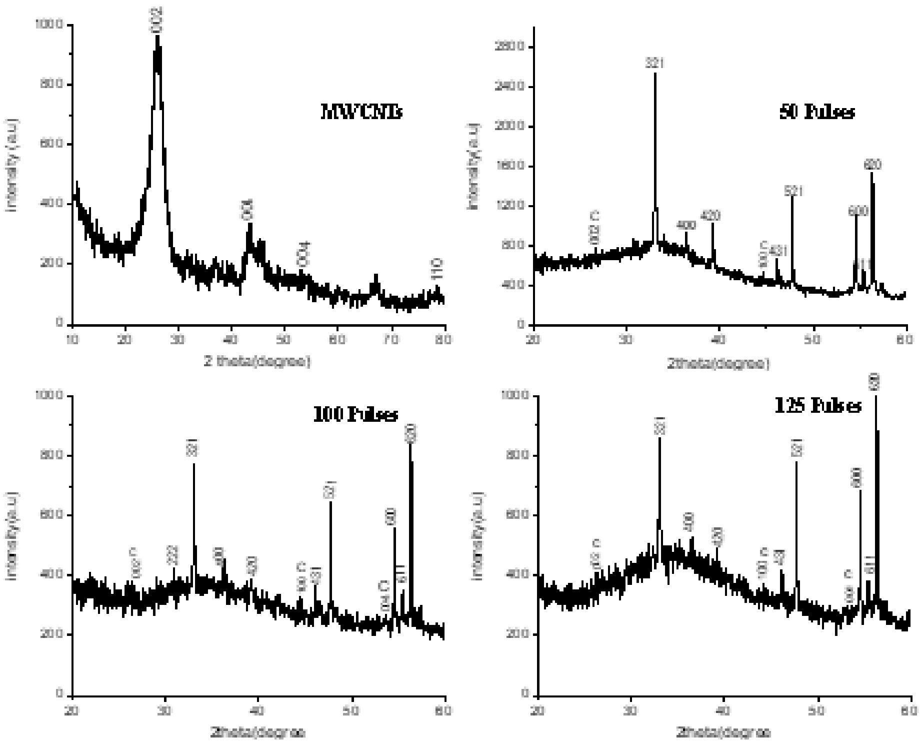

Figure 7. XRD analysis of MWCNTs and In_2O_3@MWCNTs colloidal nanoparticles prepared at 550 mJ for different pulses

Figure 8 shows the PL spectra of pure In_2O_3 nanoparticles prepared with varying laser energies for 100 shots and In_2O_3 NPs decorated MWCNTs with different numbers of laser pulses. In the visible light spectrum, In_2O_3 showed strong and sharp emission peaks centered at about 640 nm (Figure 8(a)), which are commonly attributed to oxygen deficiencies [28]. It also revealed a significant decrease in the PL emission intensity of photoluminescence spectra with increased laser energy. Such a decrease can be explained according to the improved crystalline structure of In_2O_3 NPs, as demonstrated by the XRD data, which led to a rapid decrease in oxygen vacancies and defects [29], indicating a decrease in the rate of e-h recombination in In_2O_3 NPs. However, when the laser energy reaches 650 mJ, the peak intensity of the PL emission increases. One explanation for this variation in PL intensity could be a change in the defect situation in the shallow level of the In_2O_3 NP surface.

The reconstruction of defect structures is responsible for the suppression of In_2O_3 NPs emission related to defects. These oxygen vacancies, which typically function as deep defect donors, generated a new energy level close to or inside the band gap of In_2O_3 NPs [15]. The emission peak of In_2O_3/MWCNTs nanocomposites was significantly lower than that of pure indium oxide NPs following decorating with MWCNTs in various ratios (Figure 8(b)).

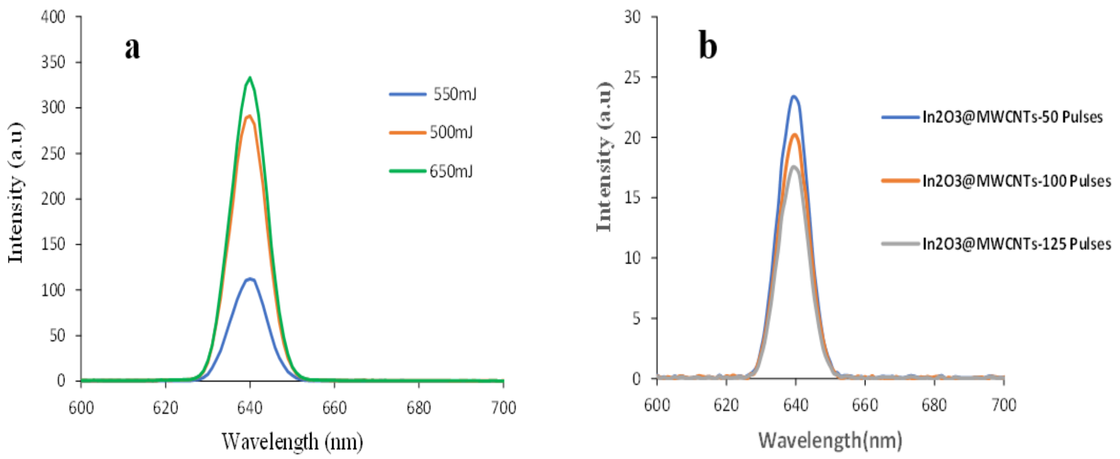

Figure 8. PL spectra of (a) pure In_2O_3 NPs prepared with different laser energies and (b) In_2O_3 decorated MWCNTs nanocomposites obtained with various laser pulses

Increased charge separation, electron-hole pair lifetime, and charge transfer into MWCNTs efficiency may be responsible for this. The prepared In_2O_3/MWCNTs nanocomposites can be used to improve photocatalytic activity and for biomedical purposes, according to PL results.

Figure 9 shows the SEM photographs with the EDX spectra of In_2O_3 NPs prepared with 550 mJ for 100 pulses and In_2O_3@MWCNTs nanocomposite synthesized with 550 mJ at 50 pulses. EDX investigation was accomplished in order to confirm the elements presented in the resulting In_2O_3 NPs and In_2O_3@MWCNTs nanocomposite, and the analysis revealed the presence of In, O, for In_2O_3 nanoparticles (Figure 9(a)). Similarly, the elemental compositions (In, O, and C) for In_2O_3@MWCNTs nanocomposite (Figure 9(b)), which emphasizes the success of the decoration process with In_2O_3 nanoparticles. The EDX spectrum also showed an additional peak that is connected to gold and is brought on by coating the samples before analysis. Also, it was proved from EDX analysis that there were no impurities in the composite indicating that the resulting nanocomposite was pure. From the SEM photographs of the inset in Figure 9, it was noted that the grain size increased and agglomerated crystallites were found within each grain and cluster with the MWCNTs addition. Additionally, irregular surface morphology was observed.

5. CONCLUSION

For the first time, we have demonstrated that MWCNTs decorated with cubic-phase indium oxide can be directly prepared by laser ablation in water. The obtained optical energy gap of In_2O_3 NPs dropped from 3.2 to 2.83 eV when decorated with MWCNT. The XRD results displayed sharp diffraction peaks and a cubic phase for In_2O_3 NPs, signifying a high degree of crystallization. It displays peaks for both In_2O_3 and MWCNT of In_2O_3@MWCNTs, confirming the notion that the addition of CNTs enhanced the mixture's crystallinity. Photoluminescence data showed that low emission peak for the In_2O_3@MWCNTs structure compared to pure In_2O_3 NPs, suggesting a low e-h pair recombination process. EDX analysis revealed the elements In, O, and C for the In_2O_3@MWCNTs nanocomposite, proving the In_2O_3 nanoparticle decoration process. Therefore, it can be concluded that MWCNTs decorated with In_2O_3 perform better in optoelectronic applications.

ACKNOWLEDGMENTS

The University of Technology in Baghdad, Iraq, provided assistance, which the authors are grateful for.

REFERENCES

[1] F. H. Rajab, R. M. Taha, A. A. Hadi, K. S. Khashan, and R. O. Mahdi, "Laser induced hydrothermal growth of ZnO rods for UV detector application," *Optical and Quantum Electronics*, vol. 55, no. 3, p. 208, Mar. 2023, doi: 10.1007/s11082-022-04473-2.

[2] K. S. Khashan and S. F. Abbas, "Indium Nitride Nanoparticles Prepared by Laser Ablation in Liquid," *International Journal of Nanoscience*, vol. 18, no. 02, p. 1850021, Apr. 2019, doi: 10.1142/S0219581X 18500217.

[3] S. A. A. Mohammed *et al.*, "Copper Oxide Nanoparticle-Decorated Carbon Nanoparticle Composite Colloidal Preparation through Laser Ablation for Antimicrobial and Antiproliferative Actions against Breast Cancer Cell Line, MCF-7," *BioMed Research International*, vol. 2022, no. 1, Jan. 2022, doi: 10.1155/2022/9863616.

[4] J. A. Saimon, S. N. Madhat, K. S. Khashan, and A. I. Hassan, "Characterization of CdZnO/Si heterojunction photodiode prepared by pulsed laser deposition," *International Journal of Modern Physics B*, vol. 32, no. 31, p. 1850341, Dec. 2018, doi: 10.1142/S0217979218503411.

[5] K. R. Reyes-Gil, E. A. Reyes-García, and D. Raftery, "Nitrogen-Doped In_2O_3 Thin Film Electrodes for Photocatalytic Water Splitting," *The Journal of Physical Chemistry C*, vol. 111, no. 39, pp. 14579–14588, Oct. 2007, doi: 10.1021/jp072831y.

[6] K. S. Khashan, A. I. Hassan, And A. J. Addie, "Characterization of CuO Thin Films Deposition on Porous Silicon by Spray Pyrolysis," *Surface Review and Letters*, vol. 23, no. 05, p. 1650044, Oct. 2016, doi: 10.1142/S0218625X1650044X.

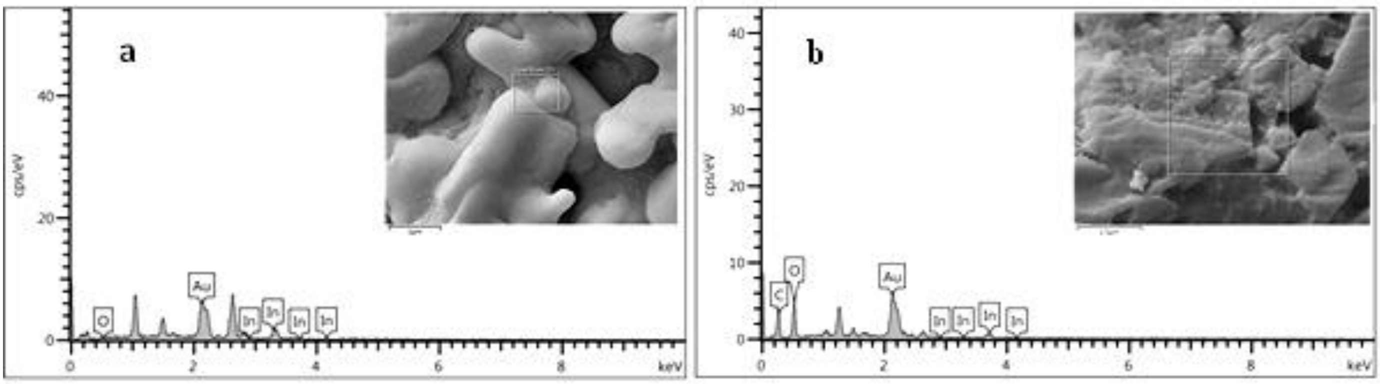

Figure 9. EDX spectra of (a) pure In_2O_3 NPs and (b) In_2O_3 NPs decorated MWCNTs. Their SEM pictures are inset

[7] S. C. Kulkarni and K.-S. Park, Y.-J. Choi, J.-G. Kang, Y.-M. Sung, and J.-G. Park, "The effect of the concentration and oxidation state of Sn on the structural and electrical properties of indium tin oxide nanowires," *Nanotechnology*, vol. 22, no. 28, p. 285712, Jul. 2011, doi: 10.1088/0957-4484/22/28/285712.

[8] A. Othonos, M. Zervos, and D. Tsokkou, "Femtosecond Carrier Dynamics in In_2O_3 Nanocrystals," *Nanoscale Research Letters*, vol. 4, no. 6, p. 526, Jun. 2009, doi: 10.1007/s11671-009-9275-0.

[9] D. S. Patil, "Effect of $Pdcl_2$ Molarity on the Gas Sensing Properties of Nanocrystalline Indium Oxide," *Sensor Letters*, vol. 13, no. 4, pp. 294–299, Apr. 2015, doi: 10.1166/sl.2015.3433.

[10] S. Guo, X. Zhang, Z. Hao, G. Gao, G. Li, and L. Liu, "In $_2O_3$ cubes: synthesis, characterization and photocatalytic properties," *RSC Advances*, vol. 4, no. 59, pp. 31353–31361, 2014, doi: 10.1039/C4RA03563A.

[11] D. Zhang *et al.*, "Ultraviolet photodetection properties of indium oxide nanowires," *Applied Physics A: Materials Science & Processing*, vol. 77, no. 1, pp. 163–166, Jun. 2003, doi: 10.1007/s00339-003-2099-3.

[12] Ch. K. Latha *et al.*, "Effect of Capping Agent on the Morphology, Size and Optical Properties of In_2O_3 Nanoparticles," *Materials Research*, vol. 20, no. 1, pp. 256–263, Jan. 2017, doi: 10.1590/1980-5373-mr-2016-0292.

[13] H. Ullah, Z. H. Yamani, A. Qurashi, J. Iqbal, and K. Safeen, "Study of the optical and gas sensing properties of In_2O_3 nanoparticles synthesized by rapid sonochemical method," *Journal of Materials Science: Materials in Electronics*, vol. 31, no. 20, pp. 17474–17481, Oct. 2020, doi: 10.1007/s10854-020-04303-9.

[14] W. H. Ho and S. K. Yen, "Preparation and characterization of indium oxide film by electrochemical deposition," *Thin Solid Films*, vol. 498, no. 1–2, pp. 80–84, Mar. 2006, doi: 10.1016/j.tsf.2005.07.072.

[15] F. A. AlMalki *et al.*, "Eco-Friendly Synthesis of Carbon Nanoparticles by Laser Ablation in Water and Evaluation of Their Antibacterial Activity," *Journal of Nanomaterials*, vol. 2022, no. 1, Jan. 2022, doi: 10.1155/2022/7927447.

[16] K. S. Khashan, A. A. Hadi, and I. F. Hasan, "Nanosecond Laser-Supported Decoration of Titanium Oxide Nanoparticles on Multiwalled Carbon Nanotubes," *Plasmonics*, vol. 19, no. 1, pp. 301–310, Feb. 2024, doi: 10.1007/s11468-023-01996-6.

[17] K. S. Khashan, B. A. Badr, G. M. Sulaiman, M. S. Jabir, and S. A. Hussain, "Antibacterial activity of Zinc Oxide nanostructured materials synthesis by laser ablation method," *Journal of Physics: Conference Series*, vol. 1795, no. 1, p. 012040, Mar. 2021, doi: 10.1088/1742-6596/1795/1/012040.

[18] Y. Li, Z. Zheng, J. Yan, B. Lu, and X. Li, "A Review on Pulsed Laser Preparation of Nanocomposites in Liquids and Their Applications in Photocatalysis," *Catalysts*, vol. 12, no. 12, p. 1532, Nov. 2022, doi: 10.3390/catal12121532.

[19] V. Duc Chinh, G. Speranza, C. Migliaresi, N. van Chuc, V. Minh Tan, and N.-T. Phuong, "Synthesis of Gold Nanoparticles Decorated with Multiwalled Carbon Nanotubes (Au-MWCNTs) via Cysteaminium Chloride Functionalization," *Scientific Reports*, vol. 9, no. 1, p. 5667, Apr. 2019, doi: 10.1038/s41598-019-42055-7.

[20] X. Cheng *et al.*, "Characterization of Multiwalled Carbon Nanotubes Dispersing in Water and Association with Biological Effects," *Journal of Nanomaterials*, vol. 2011, pp. 1–12, 2011, doi: 10.1155/2011/938491.

[21] K. Yang, M. Gu, Y. Jin, G. Mu, and X. Pan, "Influence of surface treated multi-walled carbon nanotubes on cure behavior of epoxy nanocomposites," *Composites Part A: Applied Science and Manufacturing*, vol. 39, no. 10, pp. 1670–1678, Oct. 2008, doi: 10.1016/j.compositesa.2008.07.011.

[22] N. Tripathi *et al.*, "Analysis and optimization of photonics devices manufacturing technologies based on Carbon Nanotubes," *Journal of Physics: Conference Series*, vol. 1368, no. 2, p. 022034, Nov. 2019, doi: 10.1088/1742-6596/1368/2/022034.

[23] O. K. Varghese, P. D. Kichambre, D. Gong, K. G. Ong, E. C. Dickey, and C. A. Grimes, "Gas sensing characteristics of multi-wall carbon nanotubes," *Sensors and Actuators B: Chemical*, vol. 81, no. 1, pp. 32–41, Dec. 2001, doi: 10.1016/S0925-4005(01)00923-6.

[24] N. Acacia, F. Barreca, E. Barletta, D. Spadaro, G. Currò, and F. Neri, "Laser ablation synthesis of indium oxide nanoparticles in water," *Applied Surface Science*, vol. 256, no. 22, pp. 6918–6922, Sep. 2010, doi: 10.1016/j.apsusc.2010.05.003.

[25] R. A. Ismail, "Preparation of colloidal In_2O_3 nanoparticles using nanosecond laser ablation in water," *Micro & Nano Letters*, vol. 6, no. 11, pp. 951–954, Nov. 2011, doi: 10.1049/mnl.2011.0459.

[26] V. Indora, S. Yadav, and D. Mohan, "Optical and structural analysis of sol-gel derived TiO_2/MWCNT nanocomposites," *AIP Conference Proceedings*, vol. 2220, no. 1, p. 020110, May 2020, doi: 10.1063/5.0001850.

[27] S. Mahalingam, H. Abdullah, and A. Manap, "Role of acid-treated CNTs in chemical and electrochemical impedance study of dye-sensitised solar cell," *Electrochimica Acta*, vol. 264, pp. 275–283, Feb. 2018, doi: 10.1016/j.electacta.2018.01.138.

[28] K. S. Khashan, J. M. Taha, and S. F. Abbas, "Fabrication and Properties of InN NPs/Si as a photodetector," *Energy Procedia*, vol. 119, pp. 656–661, Jul. 2017, doi: 10.1016/j.egypro.2017.07.092.

[29] J. Gan *et al.*, "Oxygen vacancies promoting photoelectrochemical performance of In_2O_3 nanocubes," *Scientific Reports*, vol. 3, no. 1, p. 1021, Jan. 2013, doi: 10.1038/srep01021.